Dynamical gap generation in a two-dimensional Dirac semimetal with a deformed Dirac cone

Hai-Xiao Xiao,[1,2] Jing-Rong Wang,[3] Hong-Tao Feng,[4] Pei-Lin Yin,[4] and Hong-Shi Zong[1,2,5,6,*]

[1]*Department of Physics, Key Laboratory of Modern Acoustics, MOE, Institute of Acoustics, Collaborative Innovation Center of Advanced Microstructures, Nanjing University, Nanjing 210093, China*

[2]*Department of Physics, Nanjing University, Nanjing 210093, China*

[3]*Anhui Province Key Laboratory of Condensed Matter Physics at Extreme Conditions, High Magnetic Field Laboratory of the Chinese Academy of Science, Hefei 230031, Anhui, China*

[4]*Department of Physics, Southeast University, Nanjing 211189, China*

[5]*Joint Center for Particle, Nuclear Physics and Cosmology, Nanjing 210093, China*

[6]*State Key Laboratory of Theoretical Physics, Institute of Theoretical Physics, CAS, Beijing 100190, China*

(Received 5 July 2017; revised manuscript received 24 August 2017; published 10 October 2017)

According to the extensive theoretical and experimental investigations, it is widely accepted that the long-range Coulomb interaction is too weak to generate a dynamical excitonic gap in graphene with a perfect Dirac cone. We study the impact of the deformation of a Dirac cone on dynamical gap generation. When a uniaxial strain is applied to graphene, the Dirac cone is made elliptical on the equal-energy plane, and the fermion velocity becomes anisotropic. The applied uniaxial strain has two effects: It decreases the mean value of fermion velocity; it increases the velocity anisotropy. After solving the Dyson-Schwinger gap equation, we show that dynamical gap generation is promoted by the former effect but suppressed by the latter. For suspended graphene, we find that the system undergoes an excitonic insulating transition when the strain is roughly 7.34%. We also solve the gap equation in case the Dirac cone is tilted, which might be realized in the organic material α-(BEDT-TTF)$_2$I$_3$ and find that the tilt of the Dirac cone can suppress dynamical gap generation. It turns out that the geometry of the Dirac cone plays an important role in the formation of excitonic pairing.

DOI: 10.1103/PhysRevB.96.155114

I. INTRODUCTION

Semimetals, no matter topologically trivial or nontrivial, have attracted intensive theoretical and experimental studies because of their intriguing properties and promising industrial applications [1–5]. Among all known semimetals, the two-dimensional (2D) Dirac semimetal plays a special role. There are two famous examples for such a semimetal: graphene [6,7] and the surface state of a three-dimensional topological insulator [8,9]. The low-energy excitations of these systems are massless Dirac fermions, described by the relativistic Dirac equation.

In contrast to normal metals that possess a finite Fermi surface, the Fermi surface of 2D Dirac semimetals shrinks to a number of discrete points at which the valence and conduction bands touch [6,7]. The Coulomb interaction between Dirac fermions remains long ranged since the density of states vanishes at the Fermi level. The influence of long-range Coulomb interaction on the low-energy dynamics of Dirac fermions has been investigated extensively [7]. Although weak Coulomb interaction is found by renormalization-group (RG) analysis to be marginally irrelevant [10–16], it gives rise to singular renormalization of fermion velocity [11–16] and logarithmiclike corrections to a variety of observable quantities, including specific heat, optical conductivity, thermal conductivity, compressibility, etc. [7]. The singular renormalization of fermion velocity has been confirmed experimentally in suspended graphene [17], quasifreestanding graphene on silicon carbide [18], and graphene on boron nitride substrates [19].

The Coulomb interaction also can induce important nonperturbative effects. Of particular interest is the possibility of a semimetal-insulator quantum phase transition that is driven by the dynamical generation of a finite excitonic gap [20–52]. Once an excitonic gap is opened, the chiral symmetry, corresponding to sublattice symmetry, is dynamically broken [7,20]. The research interest in dynamical gap generation is twofold. First, acquiring a finite gap broadens the possible applications of graphene in the design and manufacture of electronic devices [21]. Second, it is the condensed-matter counterpart of the concept of dynamical chiral symmetry breaking [53,54].

Several years before monolayer graphene was isolated in the laboratory, Khveshchenko [20] discussed the possibility of dynamical gap generation for massless Dirac fermions in 2D, motivated by the theoretical progress of dynamical chiral symmetry breaking in a (2+1)-dimensional QED. He obtained critical fermion flavors $N_f^c = 8/\pi$, above which no dynamical gap can be generated. Later, Gorbar *et al.* further studied this problem [22]. Their main results [22] are that a finite excitonic gap can be generated if the Coulomb interaction strength α, defined by

$$\alpha = \frac{e^2}{v\kappa}, \tag{1}$$

where e is the electric charge, v is the fermion velocity, and κ is the dielectric constant, is larger than some threshold α_c for a fixed fermion flavor N_f. This interesting result has stimulated extensive theoretic and numerical studies aimed at finding the precise value of α_c. Calculations performed

*zonghs@nju.edu.cn

with the Dyson-Schwinger (DS) equation [23–26,28,30], the Bethe-Salpeter equation [37,38], the RG approach [40,42], and the Monte Carlo simulation [43,44] found that the critical value α_c falls into the range of $0.79 < \alpha_c < 2.16$. For suspended graphene, the interaction strength is $\alpha \approx 2.16$, whereas for graphene placed on a SiO_2 substrate, it becomes $\alpha \approx 0.79$ [21]. It thus indicates that suspended graphene is an excitonic insulator at zero T, but graphene placed on SiO_2 remains a semimetal. However, experiments did not find any evidence for the existence of an excitonic insulating phase in suspended graphene even at very low temperatures [17,55]. In Ref. [32], the authors studied the DS equation for an excitonic gap by incorporating the wave-function renormalization, fermion velocity renormalization, and dynamical gap generation in an unbiased way and found that $\alpha_c \sim 3.2$ [32]. According to this result, the Coulomb interaction in suspended graphene is too weak to drive the semimetal-insulator phase transition. This conclusion is well consistent with experiments [55] and is confirmed by subsequent more refined DS equation studies [35,36]. In addition, recent Monte Carlo simulations [49,50] claimed that, although the Coulomb interaction in suspended graphene is not strong enough to open an excitonic gap, α_c is close to 2.16.

Although careful experiments and elaborate theoretical studies already have provided strong evidence for the absence of an excitonic gap in intrinsic graphene, there have been several proposals attempting to realize an excitonic insulator in similar semimetals. For example, it was argued that the Coulomb interaction in an organic material α-(BEDT-TTF)$_2$I$_3$ might be much stronger than graphene because its fermion velocity is about one-tenth of the one observed in graphene [56]. In addition, Triola *et al.* proposed that the fermion excitations of the surface states of some topological Kondo insulators may have extraordinary low fermion velocities, which would drive the Coulomb interaction to fall into the strong-coupling regime [57]. Moreover, it seems viable to strengthen the Coulomb interaction and as such promote the excitonic insulating transition by exerting certain extrinsic influences. Through Monte Carlo simulations, Tang *et al.* argued that applying a uniform and isotropic strain by about 15% can make the Coulomb interaction strong enough to open an excitonic gap [58].

Recently, the influence of a uniaxial strain on the properties of Dirac fermions has been studied. First-principles calculations [59,60] suggested that the uniaxial strain would cause the carbon-carbon bond to become longer along the direction of the applied strain and get shorter along its orthogonal direction. As a consequence, the originally perfect Dirac cone is deformed, and the fermion velocity along the direction of applied uniaxial strain decreases, whereas the other component of fermion velocity is made larger. Sharma *et al.* [61] investigated the possibility of dynamical gap generation in graphene with an anisotropic dispersion and argued that it is promoted by the velocity anisotropy induced by the uniaxial strain.

In this paper, we study the influence of uniaxial strain on the formation of excitonic pairing. It is important to emphasize here that applying a uniaxial strain to graphene has two effects: First, it lowers the mean value of the fermion velocity; second, it increases the velocity anisotropy, and they might have different effects on dynamical gap generation. We will address this issue by solving the self-consistent DS equation for the excitonic gap. We will show that the two effects of uniaxial strain are actually competitive since they have opposite influences on dynamical gap generation. After carrying out numerical calculations based on three widely adopted approximations, we obtain the dependence of the excitonic gap on two parameters, namely, the effective Coulomb interaction strength $\alpha = e^2/\bar{v}\epsilon$, where $\bar{v} = \sqrt{v_x v_y}$ and the velocity ratio $\eta = v_x/v_y$. We will show that the dynamical gap generation is enhanced if the mean value of fermion velocity $\bar{v}$ is lowered but can strongly be suppressed when the velocity anisotropy grows. Our conclusion is qualitatively consistent with Ref. [34]. We will present a comparison between our results and that reported in Ref. [61].

Apart from strain-induced anisotropy [59,60,62], the fermion velocity anisotropy can also be induced by introducing certain periodic potentials [63–65]. Moreover, it is found that the surface state of some topological insulators, including β-Ag_2Te [66] and β-HgS [67], is a 2D Dirac semimetal with two unequal components of fermion velocity. Our results of the impact of velocity anisotropy on dynamical gap generation are applicable to these systems.

To gain more quantitative knowledge of the effects caused by uniaxial strain, we extract an approximated expression for the fermion velocities in the x and y directions from recent first-principles calculations of uniaxially strained graphene [60]. For suspended graphene, we find that as the applied uniaxial strain grows the system undergoes a semimetal-insulator phase transition when the strain becomes larger than 7.34%. The dependence of the dynamical gap on the magnitude of the uniaxial strain is obtained from the solution of the gap equation, which shows that the gap is an increasing function of the applied strain. We thus see that the enhancement of dynamical gap generation caused by decreasing the mean velocity dominates over the suppressing effect produced by the increasing velocity anisotropy.

In addition to the uniaxial strain, the Dirac cone may be deformed in other ways. For instance, the Dirac cone is known to be tilted in an organic material α-(BEDT-TTF)$_2$I$_3$ [68–74], which is regarded as a promising candidate to realize the quantum phase transition from a 2D Dirac semimetal to an excitonic insulator [56]. We also study the fate of dynamical gap generation in such systems and show that it is suppressed when the Dirac cone is tilted.

The remaining sections of the paper are organized as follows: In Sec. II, we give the model action for the 2D Dirac fermions with anisotropic dispersion. In Sec. III, we derive the DS gap equation and then solve it by employing three different approximations. The numerical results are presented and discussed in Sec. IV. In Sec. V, we compare our results with a recent work. The direct relation between strain and gap generation is investigated in Sec. VI. The influence of the tilted Dirac cone on dynamical gap generation is studied in Sec. VII. We end the paper with a brief summary in Sec. VIII.

II. MODEL AND FEYNMAN RULES

The massless Dirac fermions with an anisotropic dispersion can be described by the action,

$$S = \int dt\, d^2\mathbf{r}\, \bar{\Psi}_\sigma(\mathbf{r})\big(i\gamma_0\partial_t - iv_x\gamma_1\nabla_x - iv_y\gamma_2\nabla_y\big)\Psi_\sigma(\mathbf{r}) - \frac{1}{2}\int dt\, dt' d^2\mathbf{r}\, d^2\mathbf{r}'\bar{\Psi}_{\sigma 1}(\mathbf{r})\gamma_0\Psi_{\sigma 1}(\mathbf{r}) \times U_0(t-t',|\mathbf{r}-\mathbf{r}'|)\bar{\Psi}_{\sigma 2}(\mathbf{r}')\gamma_0\Psi_{\sigma 2}(\mathbf{r}'). \quad (2)$$

In this action, $\Psi_\sigma^T = (\Psi_{Ka\sigma},\Psi_{K'a\sigma},\Psi_{Kb\sigma},\Psi_{K'b\sigma})$ is a four-component spinor field, representing the low-energy Dirac fermion excitations of graphene, where a and b stand for the two inequivalent sublattices and K and K' stand for two valleys. The fermion flavor $\sigma = 1,2,\ldots,N_f$ corresponds to the spin components. Although the physical flavor is $N_f = 2$, in the following analysis we will consider a generally large N_f so as to perform the $1/N_f$ expansion. The γ matrices are defined as $\gamma_{0\text{–}2} = (\tau_3, i\tau_2, -i\tau_1)\otimes\tau_3$, where $\tau_{1\text{–}3}$ are the three Pauli matrices.

If the Coulomb interaction triggers excitonic pairing, the fermions would acquire a finite mass m. This mass arises from fermion pairing, namely, $m \propto \langle\bar{\Psi}\Psi\rangle$ and usually is called a dynamically generated mass [54], which physically differs from the fermion mass m_s that is spontaneously generated via the Higgs mechanism. In the latter case, the mass m_s is determined by the vacuum expectation value of an elementary boson field ϕ, i.e., $m_s \propto \langle\phi\rangle$.

The free fermion propagator is

$$G_0(i\omega,\mathbf{k}) = \frac{1}{-i\omega\gamma_0 + v_xk_x\gamma_1 + v_yk_y\gamma_2}. \quad (3)$$

The bare Coulomb interaction between fermions is

$$U_0(t,\mathbf{r}) = \frac{e^2\delta(t)}{\kappa|\mathbf{r}|}, \quad (4)$$

where the dielectric constant is $\kappa = \epsilon_r\epsilon_0$ with ϵ_0 being the dielectric constant in vacuum and ϵ_r being a parameter determined by the substrate. After performing a Fourier transformation, we obtain the Coulomb interaction function expressed in the momentum space,

$$U_0(\mathbf{q}) = \frac{e^2}{\kappa}\int\frac{d^2\mathbf{x}}{2\pi}\frac{\exp(-i\mathbf{qr})\delta(t)}{|\mathbf{r}|} = \frac{2\pi e^2\delta(t)}{\kappa|\mathbf{q}|}. \quad (5)$$

The bare Coulomb interaction will always be dynamically screened by the collective electron-hole pairs, which is represented by the polarization function. To the leading order of the $1/N_f$ expansion, the polarization function is given by

$$\Pi(i\Omega,\mathbf{q}) = -N_f\int\frac{d\omega}{2\pi}\frac{d^2\mathbf{k}}{(2\pi)^2}\mathrm{Tr}[\gamma_0G_0(i\omega,\mathbf{k})\gamma_0 \times G_0(i\omega+i\Omega,\mathbf{k}+\mathbf{q})] = \frac{N_f}{8v_xv_y}\frac{v_x^2q_x^2+v_y^2q_y^2}{\sqrt{\Omega^2+v_x^2q_x^2+v_y^2q_y^2}}. \quad (6)$$

After including this polarization, the dressed Coulomb propagator can be written as

$$D(i\Omega,\mathbf{q}) = \frac{1}{\frac{\kappa|\mathbf{q}|}{2\pi e^2} + \frac{N_f}{8v_xv_y}\frac{v_x^2q_x^2+v_y^2q_y^2}{\sqrt{\Omega^2+v_x^2q_x^2+v_y^2q_y^2}}}. \quad (7)$$

III. DYSON-SCHWINGER EQUATION

In the presence of the Coulomb interaction, the dynamics of the Dirac fermions will significantly be affected. Generically, the dressed fermion propagator has the form

$$G(i\omega,\mathbf{k}) = \frac{1}{-i\omega A_0\gamma_0 + v_xk_xA_1\gamma_1 + v_yk_yA_2\gamma_2 + m}, \quad (8)$$

where $A_{0\text{–}2} \equiv A_{0\text{–}2}(i\omega,\mathbf{k})$ are the renormalization functions and $m \equiv m(i\omega,\mathbf{k})$ is the dynamical fermion gap. The renormalized and free propagators are connected by the DS equation,

$$G^{-1}(i\varepsilon,\mathbf{p}) = G_0^{-1}(i\varepsilon,\mathbf{p}) + \int\frac{d\omega}{2\pi}\frac{d^2\mathbf{k}}{(2\pi)^2}\gamma_0G(i\omega,\mathbf{k}) \times \gamma_0\Gamma(i\varepsilon,\mathbf{p};i\omega,\mathbf{k})D[i(\varepsilon-\omega),\mathbf{p}-\mathbf{k}], \quad (9)$$

where $\Gamma(i\varepsilon,\mathbf{p};i\omega,\mathbf{k})$ is the vertex correction. As demonstrated in Refs. [32,35,36], the functions $A_{0\text{–}2}(i\omega,\mathbf{k})$ and the vertex $\Gamma(i\varepsilon,\mathbf{p};i\omega,\mathbf{k})$ play an important role in the determination of the precise value of α_c. The purpose of the present paper is to examine whether dynamical gap generation is enhanced or suppressed by the velocity anisotropy. The qualitative impact of anisotropy actually does not rely on the precise value of α_c. For our purpose, we will retain only the leading-order contribution of the $1/N_f$ expansion to the DS equation [20,22–24] and set $A_0 = A_1 = A_2 = 1$. Under this approximation, the Ward identity requires $\Gamma = 1$. Now it is easy to find that the dynamical fermion gap $m(i\varepsilon,p_x,p_y)$ satisfies the following nonlinear integral equation:

$$m(i\varepsilon,p_x,p_y) = \int\frac{d\omega}{2\pi}\int\frac{dk_x}{2\pi}\int\frac{dk_y}{2\pi}\frac{m(i\omega,k_x,k_y)}{\omega^2+v_x^2k_x^2+v_y^2k_y^2+m^2(i\omega,k_x,k_y)}\frac{1}{\frac{|\mathbf{q}|}{(2\pi e^2)/\kappa} + \frac{N_f}{8v_xv_y}\frac{v_x^2q_x^2+v_y^2q_y^2}{\sqrt{\Omega^2+v_x^2q_x^2+v_y^2q_y^2}}}, \quad (10)$$

where

$$\Omega = \varepsilon - \omega, \quad q_x = p_x - k_x, \quad q_y = p_y - k_y.$$

An apparent fact is that the gap equations are symmetric under the transformation: $v_x \leftrightarrow v_y$. In this paper, we define the effective strength of the Coulomb interaction by $\alpha = e^2/\bar{v}\kappa$, where $\bar{v} = \sqrt{v_xv_y}$ and the velocity anisotropy as $\eta = \frac{v_x}{v_y}$ so that these two parameters, the interaction strength, and the velocity anisotropy can be adjusted separately. Now the two velocities v_x and v_y can

be reexpressed by $\bar{v}$ and η as follows:

$$v_x = \sqrt{\eta}\bar{v}, \quad v_y = \bar{v}/\sqrt{\eta}. \tag{11}$$

The above DS gap equation becomes

$$m(i\varepsilon,p_x,p_y) = \int \frac{d\omega}{2\pi}\int \frac{dk_x}{2\pi}\int \frac{dk_y}{2\pi} \frac{m(i\omega,k_y,k_y)}{\omega^2+\eta\bar{v}^2k_x^2+\frac{\bar{v}^2k_y^2}{\eta}+m^2(i\omega,k_x,k_y)} \frac{1}{\frac{|\mathbf{q}|}{2\pi\alpha\bar{v}}+\frac{N_f}{8\bar{v}^2}\frac{\eta\bar{v}^2q_x^2+1/\eta\bar{v}^2q_y^2}{\sqrt{\Omega^2+\eta\bar{v}^2q_x^2+1/\eta\bar{v}^2q_y^2}}}. \tag{12}$$

Due to the separate dependence of m on the energy and two components of momenta, it is still very difficult to solve this nonlinear integral equation numerically. In order to simplify numerical work, we will employ three widely used approximations.

Under the Hartree-Fock (HF) approximation, the polarization function in the dressed Coulomb interaction is discarded completely [38,61]. Namely, the bare Coulomb interaction actually is used. Under the HF approximation, the gap equation becomes

$$m(p_x,p_y) = \frac{1}{2}\int \frac{dk_x}{2\pi}\int \frac{dk_y}{2\pi} \frac{m(k_x,k_y)}{\sqrt{\eta\bar{v}^2k_x^2+\frac{\bar{v}^2k_y^2}{\eta}+m^2(k_x,k_y)}} \frac{1}{\frac{|\mathbf{q}|}{2\pi\alpha\bar{v}}}. \tag{13}$$

Under the instantaneous approximation, the dressed Coulomb interaction takes the form [20,22]

$$D(i\Omega,\mathbf{q}) \to D(0,\mathbf{q}). \tag{14}$$

Accordingly, the gap loses the energy dependence and depends only on the momentum. After carrying out the integration over ω, the gap equation in an instantaneous approximation is given by

$$m(p_x,p_y) = \frac{1}{2}\int \frac{dk_x}{2\pi}\int \frac{dk_y}{2\pi} \frac{m(k_x,k_y)}{\sqrt{\eta\bar{v}^2k_x^2+\frac{\bar{v}^2k_y^2}{\eta}+m^2(k_x,k_y)}} \frac{1}{\frac{|\mathbf{q}|}{(2\pi e^2)/\kappa}+\frac{N_f}{8\bar{v}}\sqrt{\eta q_x^2+\frac{q_y^2}{\eta}}}. \tag{15}$$

It is well known that dynamical screening of the polarization function plays a crucial role in the determination of the effective strength of the Coulomb interaction [26]. In an approximation proposed by Gamayun, Gorbar, and Gusynin (GGG) [26], the dynamical screening of the Coulomb interaction is partially considered. In the GGG approximation, the gap $m(i\varepsilon,\mathbf{p})$ is supposed to be energy independent, i.e.,

$$m(i\varepsilon,p_x,p_y) \to m(p_x,p_y),$$

but the energy dependence of the polarization is retained explicitly. Applying this approximation leads to

$$m(p_x,p_y) = \int \frac{d\omega}{2\pi}\int \frac{dk_x}{2\pi}\int \frac{dk_y}{2\pi} \frac{m(k_x,k_y)}{\omega^2+\eta\bar{v}^2k_x^2+\frac{\bar{v}^2k_y^2}{\eta}+m^2(k_x,k_y)} \frac{1}{\frac{|\mathbf{q}|}{2\pi\alpha\bar{v}}+\frac{N_f}{8\bar{v}^2}\frac{\eta\bar{v}^2q_x^2+(\bar{v}^2q_y^2)/\eta}{\sqrt{\omega^2+\eta\bar{v}^2q_x^2+(\bar{v}^2q_y^2)/\eta}}}. \tag{16}$$

Performing the integration of ω, the gap equation can be written further as

$$m(p_x',p_y') = \alpha\int \frac{dk_x}{2\pi}\int \frac{dk_y'}{2\pi} \frac{m(k_x',k_y')}{\sqrt{\eta k_x'^2+\frac{k_y'^2}{\eta}+m^2(k_x',k_y')}} \frac{J(d,g)}{\sqrt{(p_x'-k_x')^2+(p_y'-k_y')^2}}, \tag{17}$$

where we have employed the transformations,

$$\bar{v}p_x \to p_x', \quad \bar{v}p_y \to p_y', \qquad \bar{v}k_x \to k_x', \quad \bar{v}k_y \to k_y'. \tag{18}$$

The function $J(d,g)$ is given by

$$J(d,g) = \frac{(d^2-1)\pi - gc(d)] + dg^2c(g)}{d^2+g^2-1}, \tag{19}$$

where

$$c(x) = \begin{cases} \frac{2}{\sqrt{1-x^2}}\cos^{-1}(x), & x<1, \\ \frac{2}{\sqrt{x^2-1}}\cosh^{-1}(x), & x>1, \\ 2, & x=1, \end{cases} \tag{20}$$

and

$$d = \sqrt{\frac{\eta k_x'^2+\frac{k_y'^2}{\eta}+m^2(k_x',k_y')}{\eta(p_x'-k_x')'^2+\frac{(p_y'-k_y')^2}{\eta}}} \tag{21}$$

$$g = \frac{N_f\pi\alpha\sqrt{\eta(p_x'-k_x')^2+\frac{(p_y'-k_y')^2}{\eta}}}{4\sqrt{(p_x'-k_x')^2+(p_y'-k_y')^2}}. \tag{22}$$

IV. NUMERICAL RESULTS

We utilize the iteration method to solve the DS gap equation numerically. To ensure the reliability of the numerical results, we have chosen a series of different initial iteration values. As

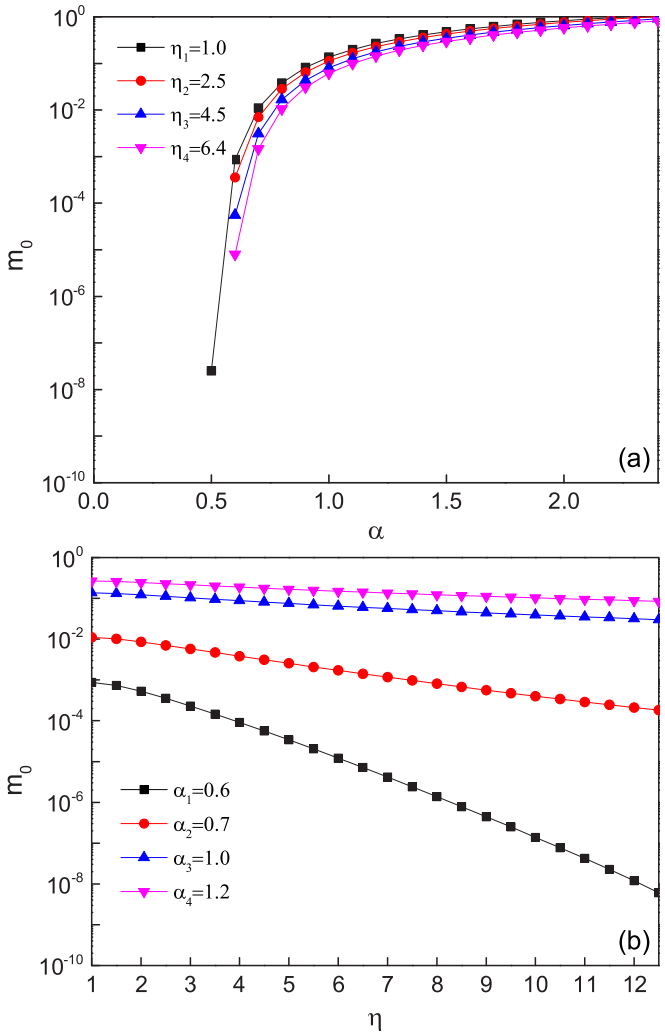

FIG. 1. (a) α dependence of m_0 for different η's; (b) η dependence of m_0 for different α's. The HF approximation is taken.

the gap equation is symmetric under $\eta \to \frac{1}{\eta}$, we only consider the case of $\eta > 1$. The energy scale we adopt here and in the following without special mention is $\bar{v}\Lambda$, and here Λ is the momentum cutoff.

A. Hartree-Fock approximation

We first consider the HF approximation. The relation between $m_0 \equiv m(0,0)$ and α obtained at a series of different values of η is displayed in Fig. 1(a). In the isotropic case with $\eta = 1$, we find that the critical value for dynamical gap generation is roughly $\alpha_c \approx 0.5$, which is consistent with Ref. [38]. According to Fig. 1(b), m_0 decreases with an increase in the fermion velocity anisotropy. As displayed in Fig. 2, in the parameter space of α and η, the semimetal phase is enlarged, but the excitonic insulating phase is compressed with the increase in the fermion velocity anisotropy. This results shows that the velocity anisotropy suppresses dynamical gap generation, which is in contrast to the conclusion reported in Ref. [61].

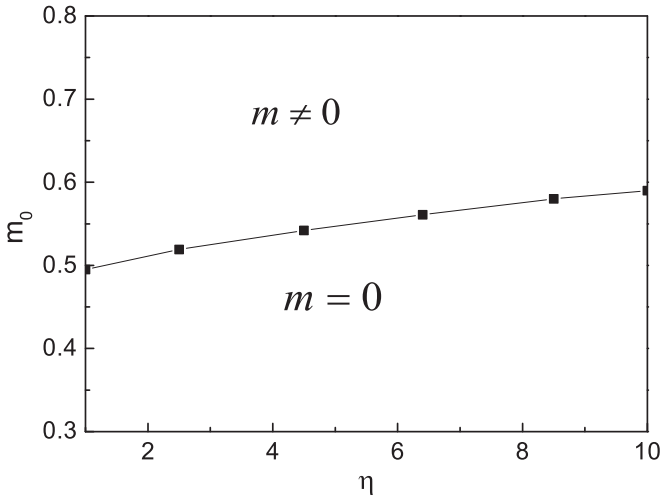

FIG. 2. Phase diagram on the α-η plane under the HF approximation.

B. Instantaneous approximation

The dependence of zero-energy gap m_0 on α is shown in Fig. 3(a) where several values of η are assumed. For $\eta = 1$, we find that $\alpha_c \approx 2.33$, which is in good agreement with previous results obtained under the instantaneous approximation [20,22]. The critical value of α_c under instantaneous approximation is obviously larger than the one under the HF approximation, which indicates that the screening from polarization suppresses the dynamical gap generation obviously. As can be observed from Fig. 3(a), m_0 increases monotonously as α grows. As η becomes larger, m_0 reduces, and α_c increases.

Then we set the value of α to study the anisotropy dependence of the excitonic mass gap. The results are shown in Fig. 3(b). As we can see, for different values of interaction strength, the increase in velocity anisotropy suppresses the formation of the dynamical generated gap. Also there is a critical velocity anisotropy η_c above which the excitonic gap dismisses.

A schematic phase diagram is depicted on the α-η plane, shown in Fig. 4. There is a critical line between the semimetal phase with vanishing m_0 and the excitonic insulating phase where $m_0 \neq 0$. This phase diagram tells us that the dynamical gap can be generated more easily by stronger Coulomb interaction and smaller velocity anisotropy.

The dependence of dynamical gap $m(p_x, p_y)$ on the momentum components $|p_x|$ and $|p_y|$ is displayed in Fig. 5. The results obtained at $\eta = 1$ and $\alpha = 2.7$ are shown in Fig. 5(a), the results obtained at $\eta = 2.5$ and $\alpha = 2.7$ are shown in Fig. 5(b), and the results obtained at $\eta = 1$ and $\alpha = 3.3$ are shown in Fig. 5(c). In the isotropic case, the gap $m(p_x, p_y)$ is symmetric under the exchange $p_x \leftrightarrow p_y$. However, as shown in Fig. 5(b), the anisotropy in fermion velocities breaks this exchange symmetry.

The momentum dependence of $m(p_x, p_y)$ exhibits the following features. In the region $\bar{v}|\mathbf{p}| > m_0$, $m(p_x, p_y)$ grows with decreasing $|\mathbf{p}|$. In the region $\bar{v}|\mathbf{p}| < m_0$, $m(p_x, p_y)$ approaches m_0 quickly with decreasing $|\mathbf{p}|$, looking nearly flat for small values of $|\mathbf{p}|$. The nearly flat region shrinks as m_0 takes a smaller value. As shown in Fig. 3(b), m_0 is suppressed

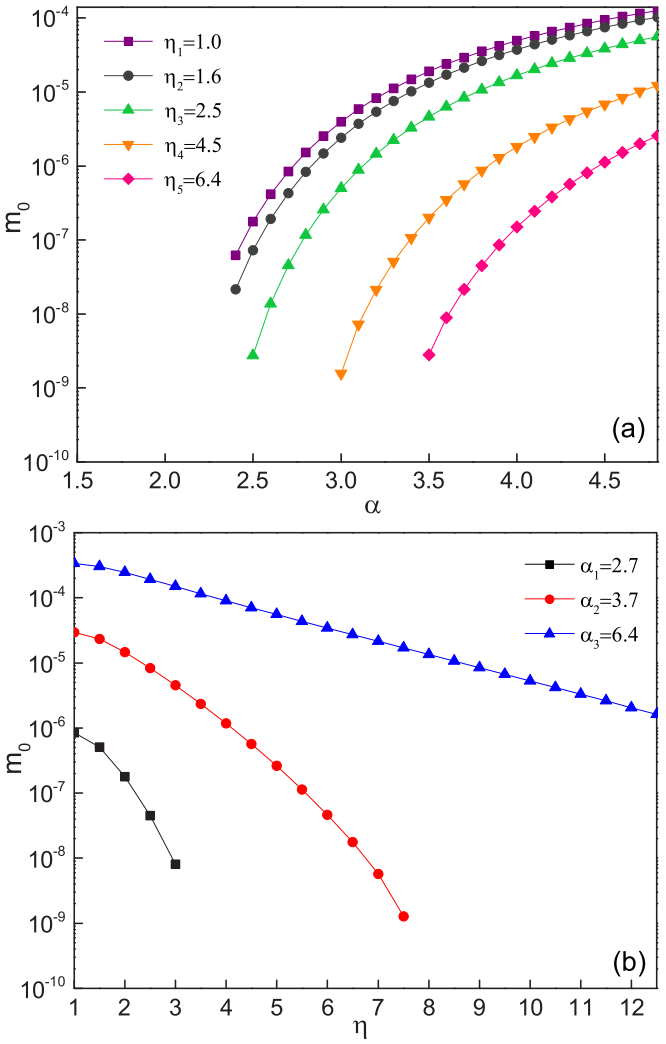

FIG. 3. (a) Dependence of m_0 on α with different η's; (b) dependence of m_0 on η with different α's. An instantaneous approximation is taken. $N_f = 2$ is taken in this figure and Figs. 4–12.

if the fermion velocity anisotropy becomes stronger, which in turn shortens the nearly flat region. Comparing Fig. 5(a) with Fig. 5(c), we see that the nearly flat region is broadened when m_0 grows as a result of the enhanced interaction strength.

In Figs. 6(a) and 6(b), we present the momentum dependences of $m(p_x = p,0)$ and $m(0,p_y = p)$ for the cases of $v_x = v_y$ and $v_x > v_y$, respectively. Comparing these two figures, we observe that the gap obtained in the anisotropic case is suppressed along both the x and the y directions comparing to the isotropic case. According to Fig. 6(b), it is easy to see that, at a given p, $m(p,0)$ is obviously smaller than $m(0,p)$ within a broad range of p.

C. GGG approximation

For several different values of η, the curves for the dependence of m_0 on the Coulomb strength α within the GGG approximation are depicted in Fig. 7(a). We can see that there is a critical interaction strength α_c above which a finite excitonic gap can dynamically be generated, the magnitude of the dynamically generated gap increases with the increase

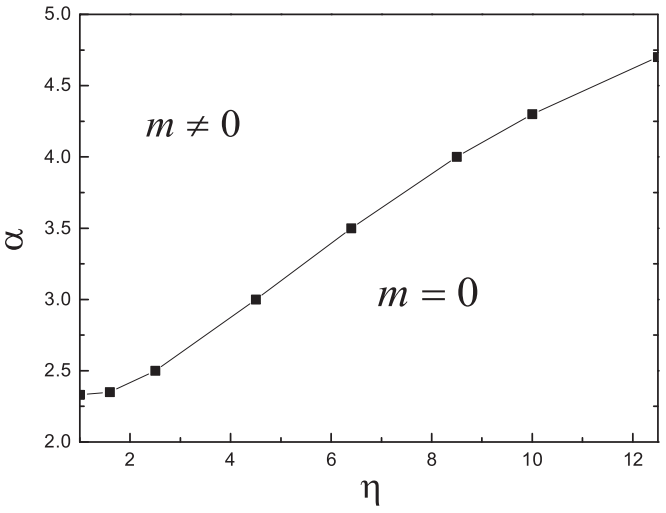

FIG. 4. Phase diagram on the α-η plane under an instantaneous approximation.

in interaction strength. It indicates dynamical gap generation appears only if the Coulomb interaction is strong enough. For the isotropic case, we get a critical interaction strength $\alpha_c = 0.92$, which is in accordance with Ref. [26]. This critical Coulomb strength is much lower than the one obtained within the instantaneous approximation $\alpha_c \approx 2.33$, which reflects that energy dependence of the dressed Coulomb interaction promotes the dynamical gap generation. As the velocity anisotropy increases, the magnitude of the dynamical gap decreases, and the critical interaction strength increases, which is consistent with the results of the instantaneous approximation.

Dependence of m_0 on the fermion velocity anisotropy η with three different values of α is presented in Fig. 7(b). It is easy to find that m_0 decreases monotonously with growing η and is suppressed completely when η is larger than a critical value.

Finally, we give the phase diagram on the α-η plane in Fig. 8. The qualitative characteristic of Fig. 8 is nearly the same as in Figs. 2 and 4. All three phase diagrams show that increasing the velocity anisotropy leads to a suppression of the dynamical gap generation.

V. COMPARISON WITH RECENT WORK

In ideal graphene, the fermions have a universal velocity v_0. Under certain circumstances, there might be an anisotropy, and the fermion velocity takes different values in different directions. For isotropic graphene, the velocity anisotropy can be induced by applying uniaxial strain or other manipulations [59,60].

In a recent work, Sharma *et al.* [61] studied the dynamical gap generation in a uniaxially strained graphene. They have introduced two parameters, namely,

$$\alpha_x = \frac{e^2}{\kappa v_x}, \tag{23}$$

and

$$\eta' = \frac{1}{\eta} = \frac{v_y}{v_x}, \tag{24}$$

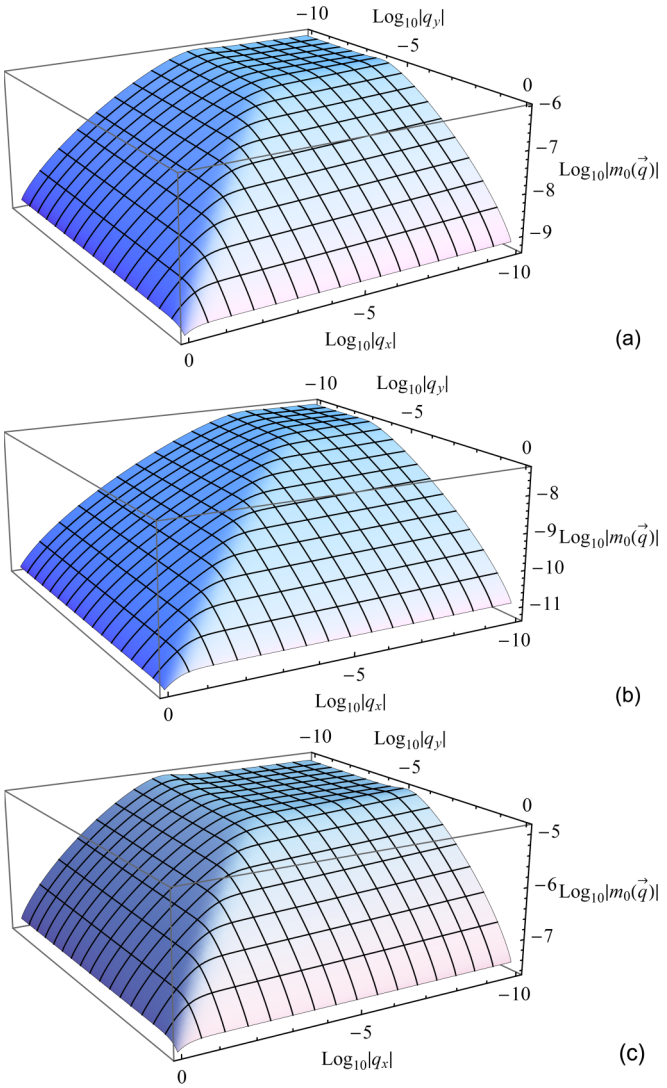

FIG. 5. Momentum dependence of the mass gap for (a) $\eta = 1$, $\alpha = 2.7$; (b) $\eta = 2.5$, $\alpha = 2.7$; (c) $\eta = 1$, $\alpha = 3.3$.

to characterize the interaction strength and velocity anisotropy. After solving the DS gap equation under the HF and instantaneous approximations, they concluded that, at a fixed α_x, the magnitude of the excitonic gap increases monotonously as the parameter η' decreases from the isotropic case of $\eta' = 1$. They also claimed that the critical value α_x^c for the dynamical gap generation decreases with deceasing η'. Based on these results, Sharma *et al.* argued that velocity anisotropy is able to promote dynamical gap generation.

We would point out that the analysis performed by Sharma *et al.* is problematic. When the parameter α_x is fixed at a certain value, the velocity component v_x also is fixed. In this case, there are actually two physical effects when lowering $\eta' = v_y/v_x$: First, the velocity component v_y decreases; second, the fermion velocity anisotropy increases. Thus the conclusion that velocity anisotropy supports the formation of excitonic mass actually is a combining effect of lowering the fermion velocity of v_y and increasing the fermion velocity anisotropy. In this sense, such a conclusion is misleading. According to our calculations, the dynamical gap generation

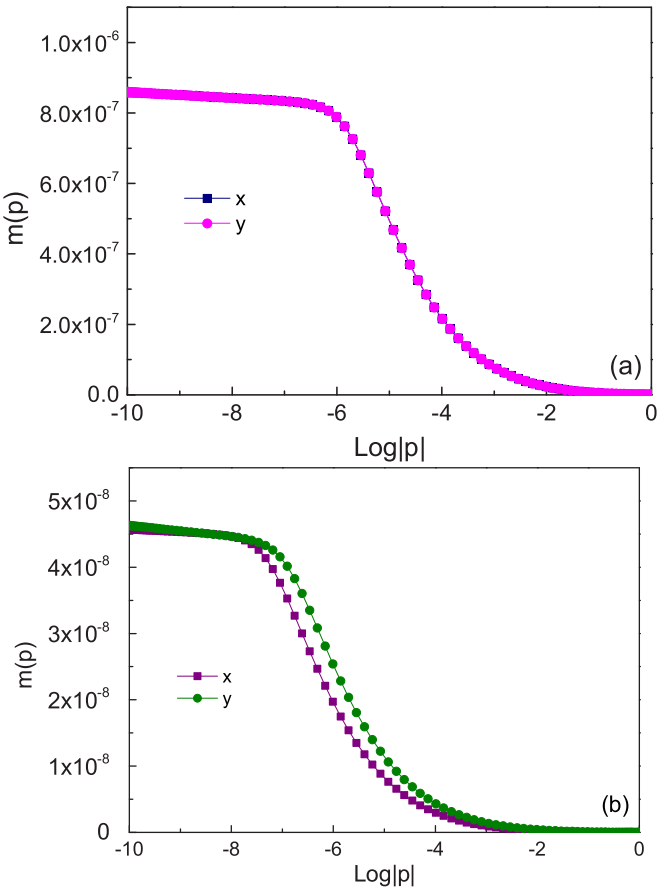

FIG. 6. Momentum dependence of $m(p)$ along the x and y directions at (a) $\eta = 1.0$ and $\alpha = 2.7$; (b) $\eta = 2.5$. $\alpha = 2.7$. Here, $m(p)$ stands for either $m(p_x,0)$ or $m(0,p_y)$.

is promoted when the mean value of the fermion velocity decreases but is suppressed as the anisotropy is enhanced. Therefore, the correct interpretation of the results obtained by Sharma *et al.* [61] should be as follows: For a fixed α_x, the promotion of the dynamical gap generation in the y direction caused by decreasing velocity is more important than the suppression caused by the growth of velocity anisotropy.

VI. EFFECTS OF UNIAXIAL STRAIN ON THE EXCITONIC GAP

The fermion velocities of uniaxially strained graphene can be obtained by performing first-principles calculations [60]. It was found [60] that the velocities in the x and y directions vary approximately linearly under uniaxial strain if the magnitude of the strain is lower than 24%. This result is valid when the strain is applied in both armchair and zigzag directions [60]. For strain $\varepsilon\%$ in the zigzag direction, we can approximate the fermion velocities with the following expressions:

$$v_x = v_0\left(1 + \frac{1}{120}\varepsilon\right), \tag{25}$$

$$v_y = v_0\left(1 - \frac{7}{240}\varepsilon\right). \tag{26}$$

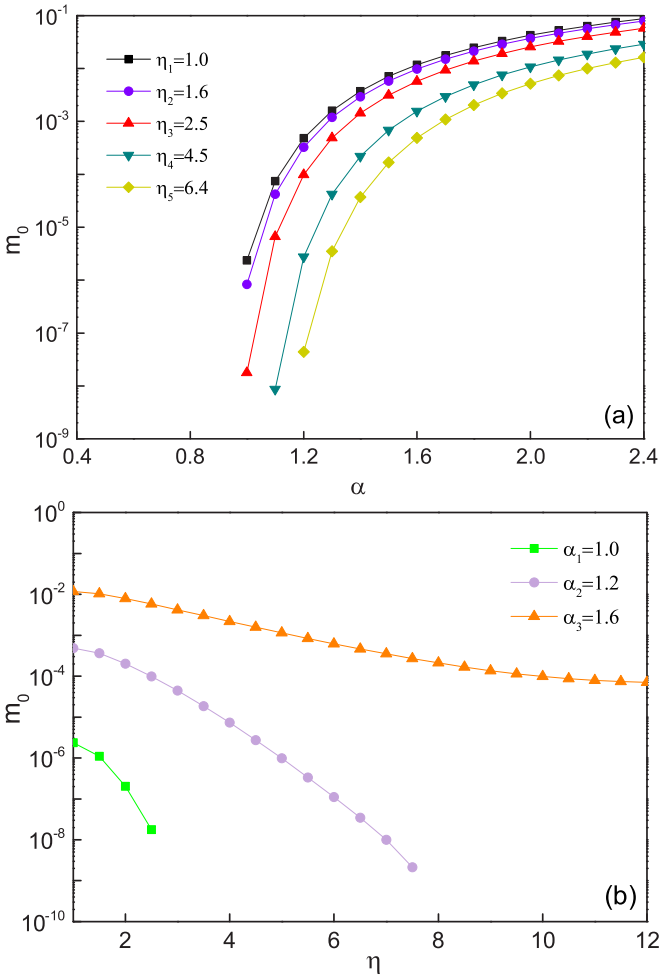

FIG. 7. (a) α dependence of m_0 for different η's. (b) η dependence of m_0 for different α's. The GGG approximation is taken.

Accordingly, the velocity anisotropy parameter η and the interaction strength α are re-written as

$$\eta = \frac{1 + \frac{1}{120}\varepsilon}{1 - \frac{7}{240}\varepsilon}, \tag{27}$$

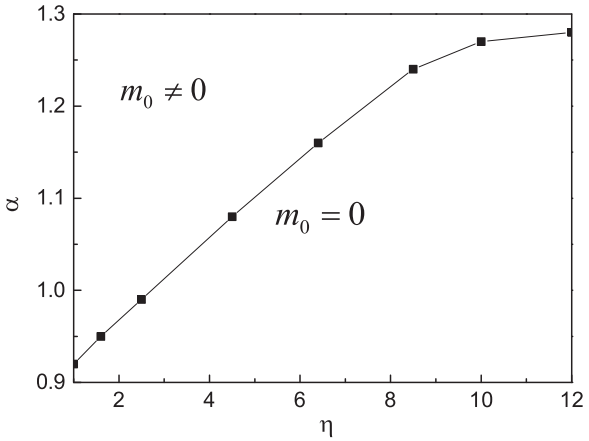

FIG. 8. Phase diagram on the α-η plane obtained under the GGG approximation.

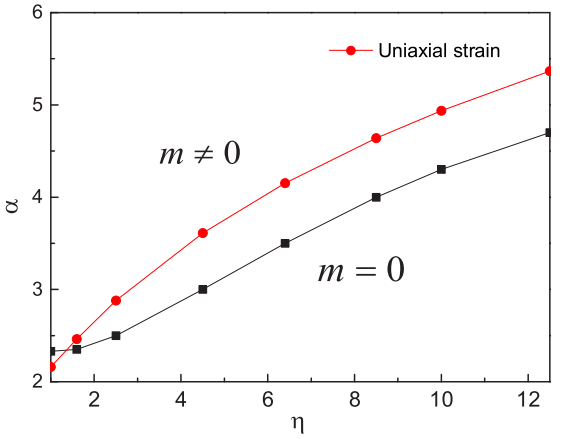

FIG. 9. Effects of uniaxial strain on interaction strength and velocity anisotropy, combined with the phase diagram on the α-η plane, obtained under the instantaneous approximation. The red line represents the trajectory of the interaction strength and velocity anisotropy of suspended graphene under uniaxial strain, and the black line stands for the critical lines of the phase transition on the α-η plane.

$$\alpha = \frac{e^2}{\kappa v_0 \sqrt{1 - \frac{5\varepsilon}{240} - \frac{7\varepsilon^2}{28\,800}}} = \alpha_0 \frac{1}{\sqrt{1 - \frac{5\varepsilon}{240} - \frac{7\varepsilon^2}{28\,800}}}, \tag{28}$$

where v_0 and α_0 are the values for graphene without strain. We suppose $\alpha_0 \approx 2.2$ for suspended graphene. It is easy to verify that both α and η increase as the strain grows. Taking advantage of these two relations and the phase diagram on the α-η plane, we obtain Fig. 9 where the red line represents the trajectory of the interaction strength and velocity anisotropy of suspended graphene under uniaxial strain, and the black line stands for the critical lines on the α-η plane within the instantaneous approximation, respectively. Here, the increase in uniaxial strain is characterized by the increase in η. It is obvious that, as the uniaxial strain increases, an excitonic gap can dynamically be generated.

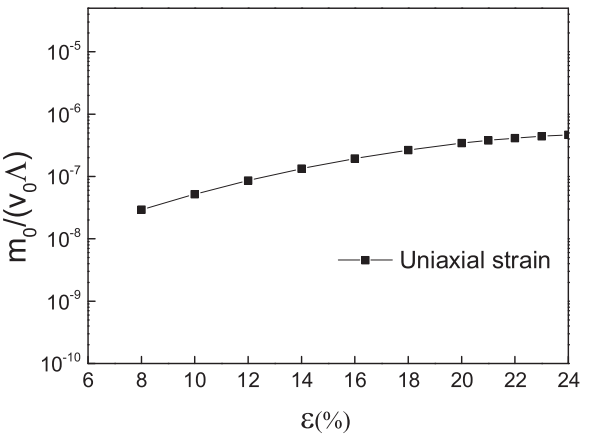

FIG. 10. Relation between the zero-energy gap m_0 and the strain parameter ε.

The relation between the dynamical gap and the strain parameter ε is presented in Fig. 10. The instantaneous approximation is employed in the calculation. In order to compare m_0 for different interaction strengths, we adopt an energy scale of the isotropic case, namely, $v_0\Lambda$ as a unit of m_0.

As we can see, the system is gapless when the uniaxial strain is smaller than 7.34%, and a finite dynamical gap is generated as ε exceeds this critical value. The zero-energy gap m_0 increases as ε grows. This implies that applying a uniaxial strain to graphene is in favor of excitonic gap generation and that the enhancement effect caused by the decreasing mean velocity dominates over the suppression effect caused by the increasing velocity anisotropy. We notice that the magnitude of dynamical gap m_0 induced by uniaxial strain is very low as clearly shown in Fig. 10. Therefore, it would be very difficult to observe such a gap in realistic materials.

VII. A 2D DIRAC SEMIMETAL WITH A TILTED CONE

It recently was argued [56] that the organic material α-(BEDT-TTF)$_2$I$_3$ might be close to a quantum phase transition between semimetallic and excitonic insulating phases due to the low fermion velocity. In the semimetallic phase of α-(BEDT-TTF)$_2$I$_3$, the Dirac cone is tilted [68–77], which can be considered a deformation of the perfect Dirac cone realized in intrinsic graphene. In this section, we examine whether the tilt of the Dirac cone favors dynamical gap generation.

The propagator of fermion excitations around a tilted Dirac cone has the form [69–74]

$$G(i\omega,\mathbf{k}) = \frac{1}{-i\omega\gamma_0 + v_t k_x\gamma_0 + v\mathbf{k}\cdot\gamma}. \tag{29}$$

We only consider the case of $v_t < v$ so that the Fermi surface still consists of discrete points. For simplicity, we assume that $v_x = v_y = v$ and focus on the influence of the tilt of the Dirac cone. The polarization is defined as

$$\Pi(i\Omega,\mathbf{q}) = -N_f \int \frac{d\omega}{2\pi}\frac{d^2\mathbf{k}}{(2\pi)^2}\mathrm{Tr}[\gamma_0 G_0(i\omega,\mathbf{k})\gamma_0 \times G_0(i\omega + i\Omega,\mathbf{k}+\mathbf{q})]. \tag{30}$$

According to Ref. [70], under the instantaneous approximation, the polarization is given by

$$\Pi(0,\mathbf{q}) = \frac{N_f}{8}\frac{|\mathbf{q}|}{v\sqrt{1-\left(\frac{v_t}{v}\right)^2\cos^2\theta_{\mathbf{q}}}} = \frac{N_f}{8}\frac{|\mathbf{q}|}{v\sqrt{1-\left(\frac{v_t}{v}\right)^2\frac{q_x^2}{q_x^2+q_y^2}}}, \tag{31}$$

here $N_f = 2$. It is then easy to get a dressed Coulomb function,

$$V(\mathbf{q}) = \frac{1}{\frac{\kappa|\mathbf{q}|}{2\pi e^2} + \Pi(\mathbf{q})} = \frac{1}{\frac{|\mathbf{q}|}{2\pi\alpha v} + \frac{N_f}{8}\frac{|\mathbf{q}|}{v\sqrt{1-\left(\frac{v_t}{v}\right)^2\frac{q_x^2}{q_x^2+q_y^2}}}}, \tag{32}$$

where

$$\alpha = \frac{e^2}{v\kappa}. \tag{33}$$

To the leading order, the gap equation is

$$m(p_x,p_y) = \int\frac{d\omega}{2\pi}\int\frac{dk_x}{2\pi}\int\frac{dk_y}{2\pi}\frac{m(k_y,k_y)}{(\omega+iv_tk_x)^2+v^2k_x^2+v^2k_y^2+m^2(k_x,k_y)}\frac{1}{\frac{|\mathbf{q}|}{2\pi\alpha v}+\frac{N_f}{8}\frac{|\mathbf{q}|}{v\sqrt{1-(\frac{v_t}{v})^2\frac{q_x^2}{q_x^2+q_y^2}}}}, \tag{34}$$

where

$$q_x = p_x - k_x, \quad q_y = p_y - k_y. \tag{35}$$

Performing the integration of ω by using the contour integral and residue theorem, we obtain

$$m(p_x,p_y) = \frac{1}{2}\int\frac{dk_x}{2\pi}\int\frac{dk_y}{2\pi}\frac{m(k_y,k_y)}{\sqrt{v^2k_x^2+v^2k_y^2+m^2(k_x,k_y)}}\frac{1}{\frac{|\mathbf{q}|}{2\pi\alpha v}+\frac{N_f}{8}\frac{|\mathbf{q}|}{v\sqrt{1-\xi^2\frac{q_x^2}{q_x^2+q_y^2}}}}, \tag{36}$$

with

$$\xi = \frac{v_t}{v}. \tag{37}$$

Here, we use ξ to measure to what extent the Dirac cone is tilted. $\xi = 0$ represents the perfect Dirac cone of graphene, and the increase in ξ stands for the increase in the tilted degree of the Dirac cone. In Refs. [69,76], an isotropic circular cutoff Λ is adopted, i.e., $|\mathbf{p}| < \Lambda$. Here, we take the momentum cutoff $\Lambda_x = \Lambda_y = \Lambda$, which means that $|p_x| < \Lambda$ and $|p_y| < \Lambda$. Moreover, we will take $v\Lambda$ as a unit of the fermion gap. Here, we would emphasize that dynamical gap generation is a genuine low-energy phenomenon and that the dominant contribution comes from small energy momenta. Although the precise value of the gap m depends on the UV cutoff, the qualitative behaviors of m and the critical coupling α_c are not sensitive to the different choices of UV cutoff.

The numerical solutions of Eq. (36) are depicted in Fig. 11, which clearly informs us that m_0 decreases with growing ξ. Therefore, the tilt of the Dirac cone reduces the possibility of dynamical gap generation. The phase diagram on the α-η plane is presented in Fig. 12.

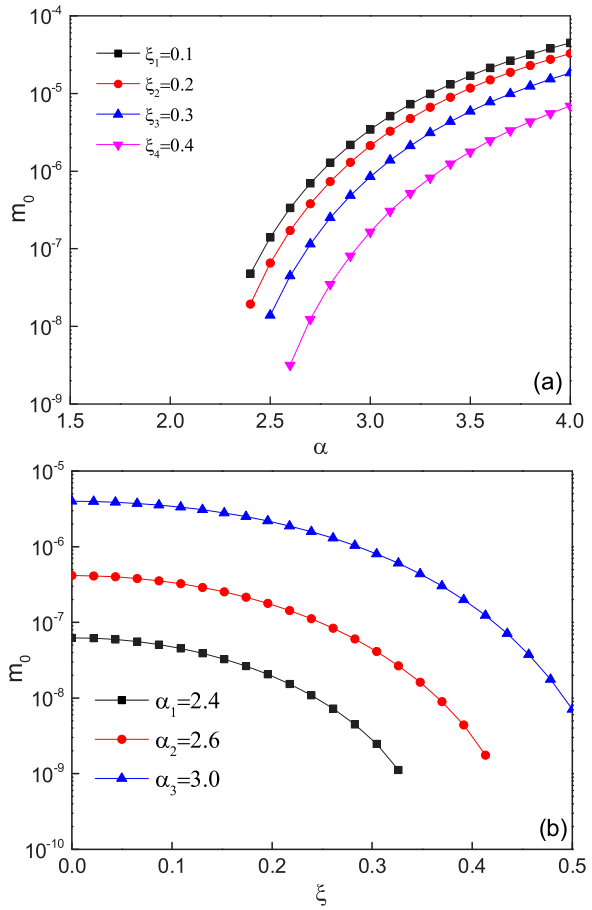

FIG. 11. (a) α dependence of m_0 for different ξ's. (b) ξ dependence of m_0 for different α's. Here, ξ is the parameter for the tilted Dirac cone.

VIII. SUMMARY AND DISCUSSION

In this paper, we have studied dynamical excitonic gap generation in a 2D Dirac semimetal with a deformed Dirac cone caused by anisotropy and a tilt of the Dirac cone. First, we studied dynamical gap generation with anisotropy, which likely is caused by uniaxial strain or periodic potentials. After solving the DS gap equation under three different approximations, we find that the decrease in fermion velocities supports dynamical gap generation but the velocity anisotropy tends to suppress dynamical gap generation. Subsequently, we have considered the organic material α-(BEDT-TTF)$_2$I$_3$, which is also a 2D Dirac semimetal, and found that dynamical gap generation is suppressed by the tilt of the Dirac cone. This shows that the shape and geometry of the Dirac cone is related closely to the formation of excitonic mass gap generation, which might help to explore concrete materials that potentially can exhibit an excitonic insulating transition.

In uniaxially strained graphene, the fermion dispersion becomes anisotropic. However, it is necessary to emphasize that uniaxial strain leads to not only velocity anisotropy, but also enhancement of an effective Coulomb interaction strength due to the decrease in the mean value of the fermion velocity. Dynamical gap generation is suppressed by the former effect but promoted by the latter one. Therefore, the ultimate influence of uniaxial strain on dynamical gap generation can only be determined by considering these two competitive effects simultaneously. The fate of dynamical gap generation depends on the actual values of α and η. By adopting the uniaxial strain dependence of fermion velocities in Ref. [60], we show that the overall effects of uniaxial strain can induce an excitonic gap in graphene once the strength of uniaxial strain is over a certain value (namely, 7.34%). This is in accordance with the results of Sharma *et al.* [61], although they have a misinterpretation of the results. It is the decrease in the fermion velocity in the direction the uniaxial strain is applied that dominates over the suppression effect caused by the growing velocity anisotropy and thus induces an excitonic gap not the velocity anisotropy contributing to the formation of excitonic gap generation.

Our analysis suggests that a more efficient way to realize the excitonic insulating transition is to merely increase the interaction strength by reducing the fermion velocity without introducing any anisotropy. For instance, one could apply a uniform and isotropic strain on graphene as suggested in Ref. [58].

Similar to other related studies [34,61,62], in this paper we assume that all the valleys have the same shape. This is a valid assumption for the usual 2D Dirac semimetals [1,2,6], including strained graphene. Of course, one cannot preclude the existence of a 2D Dirac semimetal which contains inequivalent valleys. In principle, it is possible that some Dirac cones are isotropic but other Dirac cones are anisotropic. It is also possible that the Dirac cones in a given 2D Dirac semimetal are deformed differently. A particularly interesting possibility is that a finite gap is opened only at some of the Dirac points, whereas the other Dirac points are still strictly gapless. This issue deserves further investigation.

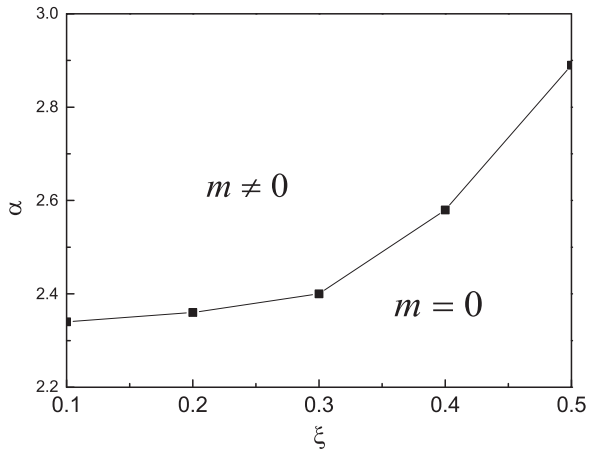

FIG. 12. Phase diagram on the α-η plane obtained under the instantaneous approximation for a 2D Dirac semimetal with a tilted cone.

ACKNOWLEDGMENTS

We thank G.-Z. Liu for valuable suggestions. This work was supported by the National Natural Science Foundation of China under Grants No. 11475085, No. 11535005,

No. 11690030, and No. 11504379, the Fundamental Research Funds for the Central Universities (under Grant No. 020414380074), the Natural Science Foundation of Jiangsu Province of China (under Grants No. BK20130387 and No. 1601170B), and the Jiangsu Planned Projects for Postdoctoral Research Funds under Grant No. 1501035B.

[1] O. Vafek and A. Vishwanath, Annu. Rev. Condens. Matter Phys. **5**, 83 (2014).
[2] T. O. Wehling, A. M. Black-Schaffer, and A. V. Balatsky, Adv. Phys. **63**, 1 (2014).
[3] H. Weng, X. Dai, and Z. Fang, J. Phys.: Condens. Matter **28**, 303001 (2016).
[4] B. Yan and C. Felser, Annu. Rev. Condens. Matter Phys. **8**, 337 (2017).
[5] M. Z. Hasan, S.-Y. Xu, I. Belopolski, and S.-M. Huang, Annu. Rev. Condens. Matter Phys. **8**, 289 (2017).
[6] A. H. Castro Neto, F. Guinea, N. M. R. Peres, K. S. Novoselov, and A. K. Geim, Rev. Mod. Phys. **81**, 109 (2009).
[7] V. N. Kotov, B. Uchoa, V. M. Pereira, F. Guinea, and A. H. Castro Neto, Rev. Mod. Phys. **84**, 1067 (2012).
[8] M. Z. Hasan and C. L. Kane, Rev. Mod. Phys. **82**, 3045 (2010).
[9] X.-L. Qi and S.-C. Zhang, Rev. Mod. Phys. **83**, 1057 (2011).
[10] R. Shankar, Rev. Mod. Phys. **66**, 129 (1994).
[11] J. González, F. Guinea, and M. A. H. Vozmediano, Nucl. Phys. B **424**, 595 (1994).
[12] J. González, F. Guinea, and M. A. H. Vozmediano, Phys. Rev. B **59**, R2474(R) (1999).
[13] D. T. Son, Phys. Rev. B **75**, 235423 (2007).
[14] J. Hofmann, E. Barnes, and S. Das Sarma, Phys. Rev. Lett. **113**, 105502 (2014).
[15] C. Bauer, A. Rückriegel, A. Sharma, and P. Kopietz, Phys. Rev. B **92**, 121409(R) (2015).
[16] A. Sharma and P. Kopietz, Phys. Rev. B **93**, 235425 (2016).
[17] D. C. Elias, R. V. Gorbachev, A. S. Mayorov, S. V. Morozov, A. A. Zhukov, P. Blake, L. A. Ponomarenko, I. V. Grigorieva, K. S. Novoselov, F. Guinea, and A. K. Geim, Nat. Phys. **7**, 701 (2011).
[18] D. A. Siegel, C.-H. Park, C. Hwang, J. Deslippe, A. V. Fedorov, S. G. Louie, and A. Lanzara, Proc. Natl. Acad. Sci. USA **108**, 11365 (2011).
[19] G. L. Yu, R. Jalil, B. Belle, A. S. Mayorov, P. Blake, F. Schedin, S. V. Morozov, L. A. Ponomarenko, F. Chiappini, S. Wiedmann, U. Zeitler, M. I. Katsnelson, A. K. Geim, K. S. Novoselov, and D. C. Elias, Proc. Natl. Acad. Sci. USA **110**, 3282 (2013).
[20] D. V. Khveshchenko, Phys. Rev. Lett. **87**, 246802 (2001).
[21] A. H. Castro Neto, Phys. **2**, 30 (2009).
[22] E. V. Gorbar, V. P. Gusynin, V. A. Miransky, and I. A. Shovkovy, Phys. Rev. B **66**, 045108 (2002).
[23] D. V. Khveshchenko and H. Leal, Nucl. Phys. B **687**, 323 (2004).
[24] G.-Z. Liu, W. Li, and G. Cheng, Phys. Rev. B **79**, 205429 (2009).
[25] D. V. Khveshchenko, J. Phys.: Condens. Matter **21**, 075303 (2009).
[26] O. V. Gamayun, E. V. Gorbar, and V. P. Gusynin, Phys. Rev. B **81**, 075429 (2010).
[27] J. Sabio, F. Sols, and F. Guinea, Phys. Rev. B **82**, 121413(R) (2010).
[28] C.-X. Zhang, G.-Z. Liu, and M.-Q. Huang, Phys. Rev. B **83**, 115438 (2011).
[29] G.-Z. Liu and J.-R. Wang, New J. Phys. **13**, 033022 (2011).
[30] J.-R. Wang and G.-Z. Liu, J. Phys.: Condens. Matter **23**, 155602 (2011).
[31] J.-R. Wang and G.-Z. Liu, J. Phys.: Condens. Matter **23**, 345601 (2011).
[32] J.-R. Wang and G.-Z. Liu, New J. Phys. **14**, 043036 (2012).
[33] C. Popovici, C. S. Fischer, and L. von Smekal, Phys. Rev. B **88**, 205429 (2013).
[34] J.-R. Wang and G.-Z. Liu, Phys. Rev. B **89**, 195404 (2014).
[35] J. González, Phys. Rev. B **92**, 125115 (2015).
[36] M. E. Carrington, C. S. Fischer, L. von Smekal, and M. H. Thoma, Phys. Rev. B **94**, 125102 (2016).
[37] O. V. Gamayun, E. V. Gorbar, and V. P. Gusynin, Phys. Rev. B **80**, 165429 (2009).
[38] J. Wang, H. A. Fertig, G. Murthy, and L. Brey, Phys. Rev. B **83**, 035404 (2011).
[39] A. Katanin, Phys. Rev. B **93**, 035132 (2016).
[40] O. Vafek and M. J. Case, Phys. Rev. B **77**, 033410 (2008).
[41] J. González, Phys. Rev. B **82**, 155404 (2010).
[42] J. González, Phys. Rev. B **85**, 085420 (2012).
[43] J. E. Drut and T. A. Lähde, Phys. Rev. Lett. **102**, 026802 (2009).
[44] J. E. Drut and T. A. Lähde, Phys. Rev. B **79**, 165425 (2009).
[45] J. E. Drut and T. A. Lähde, Phys. Rev. B **79**, 241405(R) (2009).
[46] W. Armour, S. Hands, and C. Strouthos, Phys. Rev. B **81**, 125105 (2010).
[47] W. Armour, S. Hands, and C. Strouthos, Phys. Rev. B **84**, 075123 (2011).
[48] P. V. Buividovich and M. I. Polikarpov, Phys. Rev. B **86**, 245117 (2012).
[49] M. V. Ulybyshev, P. V. Buividovich, M. I. Katsnelson, and M. I. Polikarpov, Phys. Rev. Lett. **111**, 056801 (2013).
[50] D. Smith and L. von Smekal, Phys. Rev. B **89**, 195429 (2014).
[51] F. de Juan and H. A. Fertig, Solid State Commun. **152**, 1460 (2012).
[52] A. V. Kotikov and S. Teber, Phys. Rev. D **94**, 114010 (2016).
[53] Y. Nambu and G. Jona-Lasinio, Phys. Rev. **122**, 345 (1961).
[54] V. A. Miransky, *Dynamical Symmetry Breaking in Quantum Field Theories* (World Scientific Publ., Singapore, 1993).
[55] A. S. Mayorov, D. C. Elias, I. S. Mukhin, S. V. Morozov, L. A. Ponomarenko, K. S. Novoselov, A. K. Geim, and R. V. Gorbachev, Nano Lett. **12**, 4629 (2012).
[56] M. Monteverde, M. O. Goerbig, P. Auban-Senzier, F. Navarin, H. Henck, C. R. Pasquier, C. Mézière, and P. Batail, Phys. Rev. B **87**, 245110 (2013).
[57] C. Triola, J.-X. Zhu, A. Migliori, and A. V. Balatsky, Phys. Rev. B **92**, 045401 (2015).
[58] H.-K. Tang, E. Laksono, J. N. B. Rodrigues, P. Sengupta, F. F. Assaad, and S. Adam, Phys. Rev. Lett. **115**, 186602 (2015).
[59] V. M. Pereira, A. H. Castro Neto, and N. M. R. Peres, Phys. Rev. B **80**, 045401 (2009).
[60] S.-M. Choi, S.-H. Jhi, and Y.-W. Son, Phys. Rev. B **81**, 081407(R) (2010).
[61] A. Sharma, V. N. Kotov, and A. H. Castro Neto, Phys. Rev. B **95**, 235124 (2017).

[62] A. Sharma, V. N. Kotov, and A. H. Castro Neto, Phys. Rev. B **87**, 155431 (2013).
[63] C.-H. Park, L. Yang, Y.-W. Son, M. L. Cohen, and S. G. Louie, Nat. Phys. **4**, 213 (2008).
[64] C.-H. Park, L. Yang, Y.-W. Son, M. L. Cohen, and S. G. Louie, Phys. Rev. Lett. **101**, 126804 (2008).
[65] S. Rusponi, M. Papagno, P. Moras, S. Vlaic, M. Etzkorn, P. M. Sheverdyaeva, D. Pacilé, H. Brune, and C. Carbone, Phys. Rev. Lett. **105**, 246803 (2010).
[66] W. Zhang, R. Yu, W. Feng, Y. Yao, H. Weng, X. Dai, and Z. Fang, Phys. Rev. Lett. **106**, 156808 (2011).
[67] F. Virot, R. Hayn, M. Richter, and J. van den Brink, Phys. Rev. Lett. **106**, 236806 (2011).
[68] N. Tajima and K. Kajita, Sci. Technol. Adv. Mater. **10**, 024308 (2009).
[69] H. Isobe and N. Nagaosa, J. Phys. Soc. Jpn. **81**, 113704 (2012).
[70] T. Nishine, A. Kobayashi, and Y. Suzumura, J Phys. Soc. Jpn. **79**, 114715 (2010).
[71] J. Sári, C. Toke, and M. O. Goerbig, Phys. Rev. B **90**, 155446 (2014).
[72] M. Trescher, B. Sbierski, P. W. Brouwer, and E. J. Bergholtz, Phys. Rev. B **91**, 115135 (2015).
[73] I. Proskurin, M. Ogata, and Y. Suzumura, Phys. Rev. B **91**, 195413 (2015).
[74] M. Hirata, K. Ishikawa, G. Matsuno, A. Kobayashi, K. Miyagawa, M. Tamura, C. Berthier, and K. Kanoda, arXiv: 1702.00097v2.
[75] R. Kondo, S. Kagoshima, N. Tajima, and R. Kato, J. Phys. Soc. Jpn. **78**, 114714 (2009).
[76] M. Hirata, K. Ishikawa, K. Miyagawa, M. Tamura, C. Berthier, D. Basko, A. Kobayashi, G. Matsuno, and K. Kanoda, Nat. Commun. **7**, 12666 (2016).
[77] K. Sadhukhan and A. Agarwal, Phys. Rev. B **96**, 035410 (2017).